Available online at www.sciencedirect.com
ScienceDirect
Sensors and Actuators B 129 (2008) 200–210
SENSORS AND ACTUATORS B CHEMICAL
www.elsevier.com/locate/snb

Hydrogen monitoring for power plant applications using SiC sensors

Reza Loloee [a,*], Benjamin Chorpening [b], Steve Beer [b], Ruby N. Ghosh [a,*]

[a] *Department of Physics and Astronomy, Michigan State University, E. Lansing, MI 48824, USA*
[b] *US DOE-National Energy Technology Laboratory, Morgantown, WV 26505, USA*

Received 11 July 2006; received in revised form 26 July 2007; accepted 26 July 2007
Available online 2 August 2007

Abstract

We have developed a high-temperature gas sensing system for the detection of combustion products under harsh conditions, such as an energy plant. The sensor, based on the wide band gap semiconductor silicon carbide (SiC), is a catalytic gate field-effect device (Pt–SiO_2–SiC) that can detect hydrogen-containing species in chemically reactive, high-temperature environments. The hydrogen response of the device in an industrially robust module was determined under both laboratory and industrial conditions (1000 sccm of 350 °C gas) from 52 ppm to 50% H_2, with the sensor held at 620 °C. From our data we find that the hydrogen adsorption kinetics at the catalyst–oxide interface are well fitted by the linearized Langmuir adsorption isotherm. For hydrogen monitoring in a coal gasification application, we investigated the effect of common interferants on the device response to a 20% H_2 gas stream. Within our signal to noise ratio, 40% CO and 5% CH_4 had no measurable effect and a 2000 ppm pulse of H_2S did not poison the Pt sensing film. We have demonstrated the long-term reliability of our SiC sensor and the robustness of the sensor packaging techniques, as all the data are from a single device, obtained during 5 days of industrial measurements in addition to ∼480 continuous hours of operation under laboratory conditions.

Keywords: Sensors; Hydrogen; SiC; Combustion; High temperature; Coal gasification

1. Introduction

The economic and security impact of limited natural gas supplies has reinvigorated interest in the advancement of cost-effective, clean electricity production from coal. Gasification, or the production of synthesis gas (syngas), is the first step in an advanced, minimally polluting process for production of electricity from coal known as the integrated gasification combined cycle (IGCC) power plant. An IGCC plant produces syngas from coal, cleans the syngas and supplies it as fuel to a gas turbine operated in combination with a steam turbine to maximize thermal efficiency. Future power generation systems may include fuel cells as well to achieve higher power generation efficiencies. The gasification process uses steam reforming or partial oxidation of a hydrocarbon (or a combination of the two) to produce syngas, a mixture composed mostly of hydrogen, carbon monoxide, water vapor and carbon dioxide. For optimal operation, the use of syngas in advanced power production will require online monitoring of the syngas composition via an online gas sensing system that is reliable and can survive the harsh and chemically corrosive operating conditions within the coal gasifier. The desired gas sensors must function at temperatures up to 800 °C in the presence of gases containing significant amounts of hydrogen, carbon monoxide, carbon dioxide, methane, water vapor and hydrogen sulfide. Sensitivity, selectivity, response time for real-time monitoring and long-term stability are additional essential factors for the sensing system.

The wide bandgap semiconductor silicon carbide (SiC) is an attractive candidate for these applications due to the possibility of device operation up to at least 900 °C, high thermal conductivity (4.9 W/cm K), resistance to acidic and basic species, and the maturity of the SiC device fabrication technology [1,2]. Over the past decade SiC sensors have been shown to be sensitive to automobile exhaust and flue gases, including hydrogen, hydrocarbons, CO and NO_x [3–6]. Depending on the application various authors have used different semiconductor device structures such as capacitors, Schottky diodes, p–n diodes and field-effect transistors [1,2,7,8]. We have chosen to use an n-type metal–oxide–semiconductor (MOS) capacitive device on SiC as the high-temperature gas sensor. The sensor is a cat-

* Corresponding authors.
E-mail addresses: loloee@pa.msu.edu (R. Loloee), ghosh@pa.msu.edu (R.N. Ghosh).

0925-4005/$ – see front matter © 2007 Elsevier B.V. All rights reserved.
doi:10.1016/j.snb.2007.07.118

alytic gate field-effect device (Pt–SiO_2–SiC) that can detect hydrogen-containing species with ms resolution at 620 °C [9].

This paper is divided into two sections. First we present the result from our sensors operating under laboratory conditions with a sensor temperature of 620 °C and a room temperature gas flow. These measurements were made in a test bench at Michigan State University. We used five different concentrations of hydrogen gas (10.1%, 0.984%, 0.201%, 508 and 52.1 ppm, all with N_2 balance) as the reducers and 1.01% oxygen as the oxidizer (with N_2 balance). In the second part, we tested the performance of the sensor system in an industrial environment, with conditions nearer to those in a syngas facility. These measurements were made in the high performance reactor (HPR) facility at the Dept. of Energy's National Energy Technology Laboratory (DOE-NETL) in Morgantown, WV. We examined the response and selectivity of the sensor in a wide range of syngas composition, including a range of H_2 gas concentration (up to 50%) and common interferant gases such as CO, CO_2, CH_4 and H_2S. In this case the gas temperature was about 350 °C with a 1000 sccm gas flow rate. The sensor temperature was maintained at 620 °C, as in the laboratory experiments. The sensor was self-heated to a temperature far above that of the gas under interrogation for two reasons: first, to ensure that the sensor response would not be affected by fluctuations in the gas temperature and second to obtain a fast (ms) response to changes in flow composition.

The response of the Pt–SiO_2–SiC sensor to hydrogen is a multistep process. Following dissociation of molecular hydrogen at the heated Pt catalytic sensing film, atomic hydrogen diffuses through the catalyst and is adsorbed at the metal–oxide interface creating a dipole layer, which in turn shifts the device potential by an amount, ΔV. For our capacitive structures we fix a capacitance set-point and monitor the chemically induced change in potential as the sensor signal. The kinetics of hydrogen adsorption at the metal–insulator interface has been studied both experimentally and theoretically by a number of groups [10–17]. Standard models of the sensor response, ΔV, invoke an adsorption isotherm to determine the number of occupied adsorption sites. These include the Temkin isotherm [15], which predicts a logarithmic relationship between sensor signal and hydrogen concentration (typically in the 0–10% range) and the Langmuir isotherm [18]. Here we examine the applicability of both isotherms in terms of the hydrogen response of our sensor to a room temperature and 350 °C flowing gas stream.

2. Experimental

2.1. Sensor fabrication, characterization and measurement

The SiC field-effect gas sensors were fabricated on n-type 6H–SiC substrates with a 5 μm epitaxial layer (nominal doping of 2.1×10^{16} N/cm^3), grown on 3.5° miscut, highly doped (5×10^{18} N/cm^3) wafers. The gate oxide (~39 nm) was grown on 1 cm^2 SiC chips via dry oxidation at 1150 °C, followed by a 900 °C Ar anneal and a 2 h 1175 °C post-oxidation NO passivation anneal [19]. The Pt gates (100 nm thick) were sputtered directly onto the SiO_2–SiC chips using a dc magnetron sputtering at a substrate temperature of 350 °C and in a 2.5 m Torr Ar

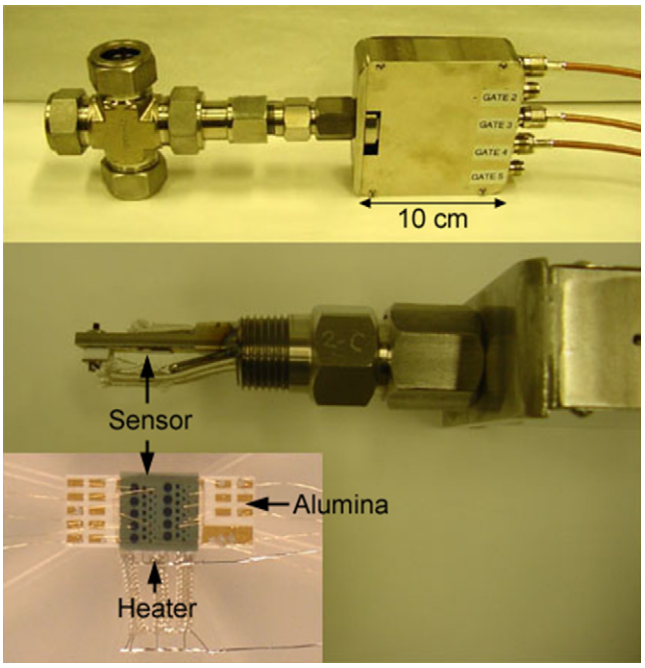

Fig. 1. Photographs of: (i) top panel—sensor test module with the electrical breakout box and (ii) bottom panel—the interior of the test module with a SiC sensor chip. Shown in the insert is the array of 52 sensors on a 1 cm^2 SiC chip mounted on an alumina header with three backside heaters.

atmosphere. Using a mechanical mask, we deposited an array of 52 gates (see Fig. 1 insert) on each chip with nominal diameters ranging from 200 to 1000 μm. Each chip was then glued onto a thermally conducting, electrically insulating alumina header using silver print. After connecting the Pt gates to the gold pads on the alumina header via wire bonding, the whole assembly was mounted inside a high-temperature sensor test module. The mounted chip can be heated up to 670 °C by three microheaters attached to the back of the alumina header.

Each Pt–SiO_2–SiC sensor was characterized via 1 MHz capacitance–voltage spectroscopy at 300–620 °C using a Boonton capacitance-meter (model 7200) with sensitivity of 1 pF. Details of the sample preparation and measurement techniques are in Ref. [20]. The C–V curves were taken under (i) ambient conditions, 99.999% purity mixtures of (ii) 1.01% oxygen in nitrogen and (iii) 10.1% hydrogen in an 80 sccm nitrogen gas stream. Prior to sensing measurements, the Pt catalytic gate was activated [2]. Activation took place by switching back and forth between oxidizing and reducing gases for several hours at a sensor temperature ≥620 °C. This procedure is required to obtain a fast and stable sensor response. All the devices on the 1 cm^2 sensor chip were activated simultaneously by flooding the entire chip with gas.

To use the device as a sensor, we use a feedback circuit to hold the capacitance constant, and monitor the gate bias voltage during gas exchange as the sensor signal [3]. We have developed a sensor control and data acquisition program for sensing measurements at industrial application sites that runs as an executable on any personal computer with a National Instruments GPIB data acquisition card. A graphical user interface allows the operator to choose the (i) sensor set-point or capacitance set-

point, (ii) slope or first order control parameter for the control algorithm to maintain the sensor at a specific capacitance during gas exchange, (iii) time delay between measurement (minimum is 5 ms), (iv) gliding average and feedback delay which determine the noise and stability, respectively of the measured signal and (v) bias limits to prevent damage to the sensor. The data is displayed on an oscilloscope-like screen in real time as well as saved in a text file along with the experimental conditions.

2.2. Industrially robust sensor test module

We have designed and fabricated a sensor test module (see Fig. 1) that is compatible with harsh industrial conditions. The module together with the electrical breakout box and the Swagelock union cross can be connected to a pressurized, high-temperature reactor, such as the HPR microreactor at NETL. The "lava" sealant inside the Conax Buffalo connector provides a thermal barrier for the hot (200–550 °C) gas as well as a preventing leakage of the hot gas into the electrical breakout box. Five independent sensors on the SiC chip and the heater array can be accessed through the electrical breakout box along with the heater leads. The electrical connection between the external coaxial cables and the (i) gold pad on the alumina sensor holder were made with nickel–chromium 80/20 wire with a fiberglass sleeve for electrical isolation and (ii) two 0.079 cm diameter Pt wires for the heater assembly. The coaxial connectors and coaxial cables are rated for continuous operation at 200 °C. Although the last 20 cm of wiring to the sensor are not coaxial leads, we are able to measure the device capacitance to better that ±1 pF in a hot gas stream.

This industrially robust module with a mounted SiC sensor chip was shipped via commercial carrier to the test site and was installed on the exhaust of the high performance reactor by the facility technician. The HPR, normally used for the study of partial oxidation chemistry [21], is supplied reactant gases through an array of gas flow lines with electronically controlled pneumatic valves and mass flow controllers, supervised by industrial control software. The gas flow chart is shown in Fig. 2. Incoming gases flow through a 700 °C furnace, housed inside a conditioning box maintained at 200 °C. The exhaust gas leaving the conditioning box through a 1/4 in. stainless steel tube was connected to the union cross of the test assembly. As the SiC sensor was located about 30 cm from the conditioner, electrical heating tape and insulation were wrapped around the 1/4 in. tubing coming into the sensor, the union cross and the gas line returning to the conditioner to maintain the gas temperature. The gas temperature inside the union cross, approximately 1 cm upstream from the SiC sensor was monitored with a type K thermocouple. Due to heat losses, measurements during a week long run were limited to a gas temperature of 350–370 °C in this set-up. The SiC sensor itself was heated to 600 or 620 °C using the microheaters on the alumina header during all the measurements to maximize the magnitude and response time of the sensor signal. Note that the gas exchange time in the vicinity of the sensor is not instantaneous. This is because the sensor is located in one arm of the Swagelok 1 in. union cross (~4 cm from the center of the cross), with either 80 or 1000 sccm of heated gas flowing in and

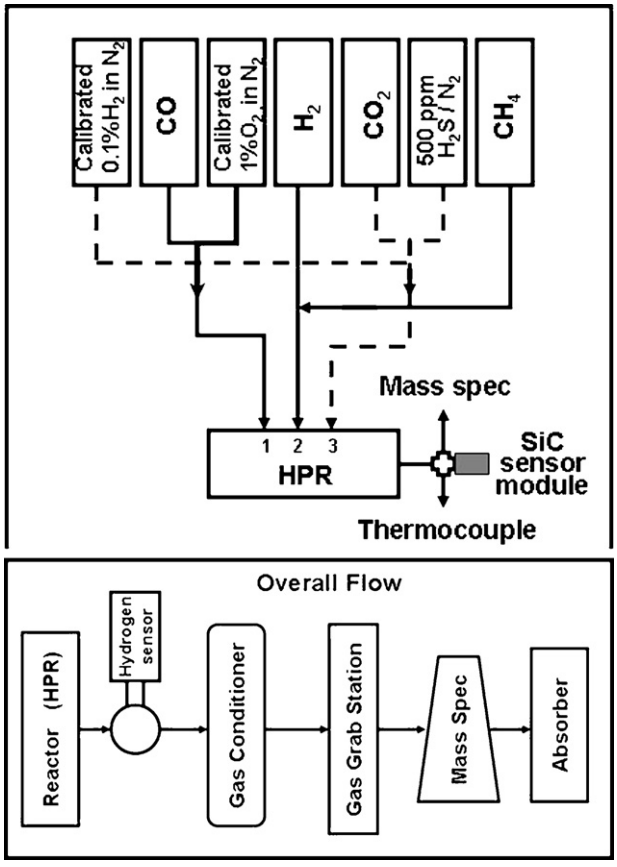

Fig. 2. Schematic of the industrial high performance reactor gas flow system. CO and calibrated 1% O_2 share input #1, pure H_2 and CH_4 share input #2, while calibrated 1%H_2, CO_2 and H_2S share input #3.

out through the adjacent arms. The resulting sidearm volume housing the sensor is less than 15 cm^3. Based on the response of the sensor to changes between reference mixtures, we estimate that it takes up to a few minutes to completely exchange the gas in the sidearm containing the sensor.

An in-line mass spectrometer located about 13 m downstream from the SiC sensor was used to validate the sensor data. The difference in location between the SiC sensor and the mass spec resulted in ~2 min of lag time between the responses of the two instruments. Time synchronized data from the industrial control software (controller for all gas lines, mass flow controllers and the thermocouple output), mass spectrometer and SiC sensor data acquisition software were collected. The data presented here has been corrected for the time lag between the various instruments. In addition note that as nitrogen is used for the balance gas for all sensing measurements, the nitrogen signal is not shown in any of mass spectrometer data.

3. Results

3.1. Laboratory measurements with room temperature hydrogen

3.1.1. Electrical characterization at high temperature

Prior to measurements under industrial operation conditions, all devices on the sensor chip were fully electrically

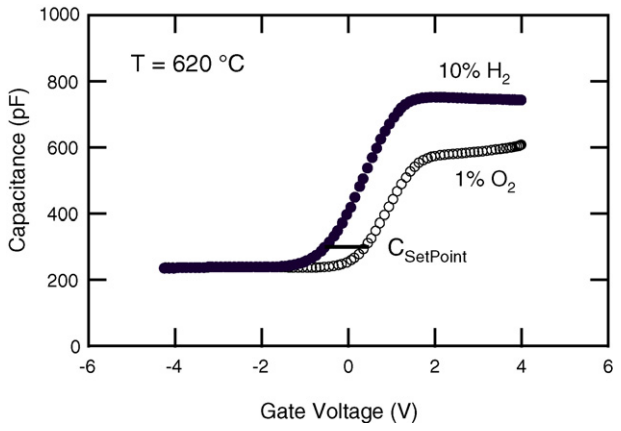

Fig. 3. Capacitance–voltage characteristic (1 MHz) of a SiC gas sensor at 620 °C in 10.1% H_2 and 1.01% O_2 (balance N_2) taken with a 400 mV/s sweep rate from positive to negative bias. The device is a Pt–SiO_2–SiC n-type capacitor with a 1000 μm diameter catalytic Pt sensing film.

characterized and their response to room temperature hydrogen gas was determined. For the sensing measurements, the appropriate sensor set-point was determined from the 1 MHz capacitance–voltage curves at 620 °C in hydrogen (10.1%) and oxygen (1.01%) environments shown in Fig. 3. This device has a sensing film or Pt catalytic gate, 100 nm in thickness and 1000 μm in diameter. For reliable high-temperature operation, we have previously determined that the optimum sensor biasing condition (capacitance set-point) is near mid gap capacitance [3,20]. This determination is, based on a detailed understanding of the hydrogen transduction mechanisms of the sensor, discussed further in Section 3.2.

Robust, long-term sensor operation at temperatures above 600 °C places stringent demands on the sensor structure as well as the associated signal measurement leads or electrical connections. Evidence of the reliability of our device fabrication and mounting process is given by the fact that all the data presented in this paper comes from a single 1 mm diameter gate which operated for ∼40 h of measurement in the industrial setting and during more than 400 h of continuous measurement in the laboratory. Note that these particular laboratory measurements were performed after exposure to H_2S in the HPR reactor. Although four additional gates on the chip were always available for measurement, they were simply not needed for our experiments. We have achieved this level of reliability by carefully tuning our sensor fabrication process. The two key components are first the high-temperature reliability of the oxide [22] which was achieved by optimization of the oxide growth [19], and secondly the development of a Pt sensing film can withstand repeated thermal cycling as well as extended high-temperature exposure while maintaining its properties as a catalyst [20]. The robustness of the signal transmission path was ensured by developing a reliable technique for each and every electrical connection such as wire bonding to the sensing film, attachment of the nichrome lead to the alumina header. No failures of any of the electrical connections within the test module were observed during these measurements.

3.1.2. Sensor measurements with room temperature hydrogen

To determine the hydrogen response of our devices, we initially selected five gates, one of every size on the chip (200, 300, 500 and 1000 μm in diameter). Under laboratory conditions we measured the sensor response to 10.1%, 0.984%, 0.201%, 508 and 52.1 ppm H_2 with N_2 as the balance gas. In each case 1.01% O_2 was used as the reference gas. A sensor temperature of 620 °C was selected for all of these atmospheric condition measurements to maximize both the magnitude and speed of the sensor response [22]. All the measured gates on this chip gave similar results; in this paper we present data from a single 1000 μm Pt gate or sensor for the laboratory and industrial experiments. Note that the sensor signal itself does not depend on gate area. The advantage of using the largest gate is that the signal to noise ratio (S/N) is proportional to the slope of the capacitance–voltage curve (Fig. 3) at the set-point ($C_{set\text{-}point}$), so a larger gate has a larger S/N ratio.

The sensor signal as a function of H_2 gas concentration with three cycles at each gas composition is shown in Fig. 4. The exposure time in H_2 and O_2 were 200 and 300 s, respectively. The device response is reproducible over 3.5 decades of hydrogen concentration. The repeatability of the sensor signal is ±2%, based on a comparison of the first and last set of cycles in 10.1% H_2. The ultimate sensitivity of the sensor is not known at present. At the time of the measurement, the lowest hydrogen concentration available in our laboratory was 52.1 ppm. From the S/N ratio of the data in Fig. 4, clearly lower concentration measurements are possible. Note that the observed response time of ∼0.5 min to hydrogen and ∼2 min to oxygen is not the intrinsic response time of the sensor, but the gas exchange time of the system, which we estimate to be on the order of a few minutes. We have previously shown that the intrinsic sensor response time

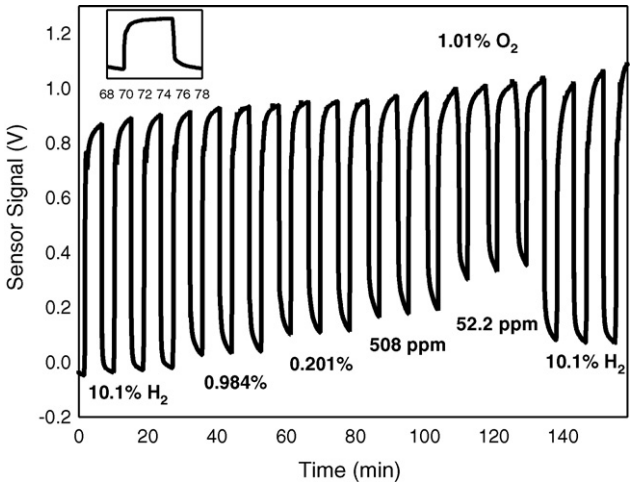

Fig. 4. Sensor measurements on a 1000 μm Pt gate (sensing film) from a SiC sensor chip. The sensor temperature was 620 °C with the room temperature gas flowing at 80 sccm. 1.01% O_2 was used as the reference gas. Shown are three complete cycles in 10.1%, 0.984%, 0.201%, 508 and 52.1 ppm H_2. The sensor responds to hydrogen over at least 3 1/2 decades of hydrogen concentration. The repeatability of the measurement, comparing the first and last 10.2% H_2 cycles is better than 2%. Insert: single cycle of the sensor response to 0.201% H_2 and 1.0% O_2.

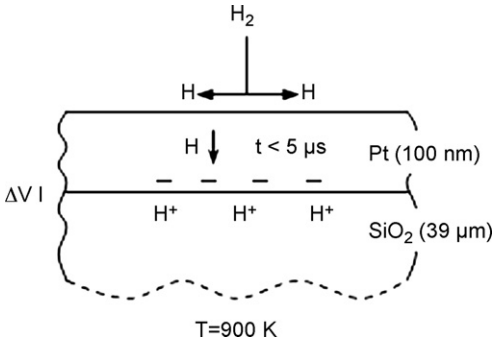

Fig. 5. Schematic of hydrogen transduction in a metal–oxide–semiconductor field-effect sensor.

is ∼1 ms [9], in a different set-up where gas is injected from a small nozzle directly onto the 1 mm diameter sensor film. A short gas exchange time was achieved by restricting the volume to be exchanged to only 1 μL.

3.1.3. Response mechanisms of Pt–SiO_2–SiC sensor to hydrogen

The response of catalytic gate Pt–SiO_2–SiC field-effect sensors to hydrogen is a multistep process as shown in Fig. 5. First, molecular hydrogen dissociates at the heated Pt sensor film or gate of the capacitor. Secondly, atomic hydrogen diffuses rapidly, $\tau < 5$ μs for a 100 nm Pt film at $T > 430\,^{\circ}$C [23], through the Pt gate and is adsorbed on sites at the metal–oxide interface. A dipole layer builds up at the Pt–SiO_2 interface with the negative charge in the metal and the protons in the oxide [14], shifting the potential of the MOS capacitor towards negative bias. The sensor signal is obtained by monitoring the chemically induced shift in device potential as a function of hydrogen concentration. In our case we fix the sensor bias near mid-gap capacitance and monitor the voltage needed to maintain that capacitance as the sensor signal, while modulating the hydrogen concentration. We have previously shown that for metal–oxide–semiconductor (MOS) sensors, fast reproducible sensor responses require a careful choice of sensor set-point, in our case near mid-gap capacitance [3,9].

The resultant potential change (ΔV) is the steady state response of the sensor to a particular hydrogen concentration. Experimentally we obtain the sensor response by comparing the signal in hydrogen to the signal in a completely oxidizing environment; consequently ΔV is proportional to the number of adsorbed atoms at the metal–insulator interface. Standard models of the response of electrochemical sensors invoke an adsorption isotherm to determine the concentration of adsorbed atoms at this interface for different gas concentrations or pressure. We briefly describe two of the isotherms we will use to compare to our data, the Temkin and Langmuir isotherms.

The most commonly used isotherm in the field is the Temkin isotherm that assumes that the heat of adsorption ΔH decreases with decreasing coverage (θ), where θ is a measure of the number of occupied adsorption sites. In our case θ is proportional to ΔV. The Temkin isotherm predicts a linear relationship between sensor response and the logarithm of the hydrogen pressure [15]:

$$\Delta V \propto \theta \propto RT \ln(P_{H_2}) \tag{1}$$

where R is the universal gas constant and T is the temperature in Kelvin. The Temkin isotherm is primarily valid under ultra high vacuum (UHV) conditions with low to medium coverage [15,16].

A second very general isotherm, that is applicable for a wide variety of interactions between molecules and an adsorptive surface, is the linearized Langmuir isotherm. This isotherm, which makes fewer assumption than Temkin, can be expanded to include dissociative adsorption under the condition that: (i) the solid surface is made up of a uniform array of energetically identical adsorption sites, (ii) the adsorbates constitute only a single layer (monolayer) on the surface and (iii) the adsorption and desorption rate is independent of the population of neighboring sites. The linearized Langmuir isotherm for dissociative adsorption can be written in its final form as

$$\frac{\sqrt{x}}{v} = \frac{1}{cv_m} + \frac{\sqrt{x}}{v_m} \tag{2}$$

where x is the hydrogen pressure (here H_2%), v the volume of adsorbed gas (here $v \propto \Delta V$), v_m the maximum value for v and c is the temperature dependent adsorption equilibrium constant which is related to the adsorption free energy.

3.1.4. Sensor response to room temperature hydrogen gas

The steady state response of the sensor (ΔV) to a series of hydrogen pulses (Fig. 4) is shown in Fig. 6. The sensor response, ΔV (H_2%) for a given hydrogen concentration in percent (balance is N_2) is obtained from the difference in the asymptotic value of the sensor signal in 1.01% oxygen versus that in hydrogen and represents the average value of ΔV from three complete cycles. Note that the error bars are smaller than the symbols. We first fitted our data to the Temkin isotherm by plotting the sensor response as a function of the logarithm of the hydrogen concentration in Fig. 6a. This procedure gives a slope of 84.8 ± 4 mV/decade with a correlation of $R = 0.98608$. There is a slight scatter in the data, and a hint that the response may be saturating about 10.1% H_2. We then fitted the same data to the Langmuir isotherm, using Eq. (2) to plot the quantity $\sqrt{H_2\%}/\Delta V$ versus $\sqrt{H_2\%}$, obtaining a slope of 1.0872 ± 0.0006 and an intercept of 0.0032 ± 0.0006 with a correlation of $R = 0.99992$. The Langmuir isotherm is an excellent fit to our experimental data.

3.2. Harsh, industrial environment measurements

Our laboratory measurement system is dedicated for measurements at only low hydrogen concentrations in the 52 ppm to 10% range for a room temperature gas flow. The HPR reactor at NETL allowed us to study higher hydrogen concentrations as well as the effect of interferent gases such as CO, CO_2, CH_4 and H_2S. In addition we were able to operate our sensors at higher flowing gas temperatures that are closer to realistic energy plant conditions.

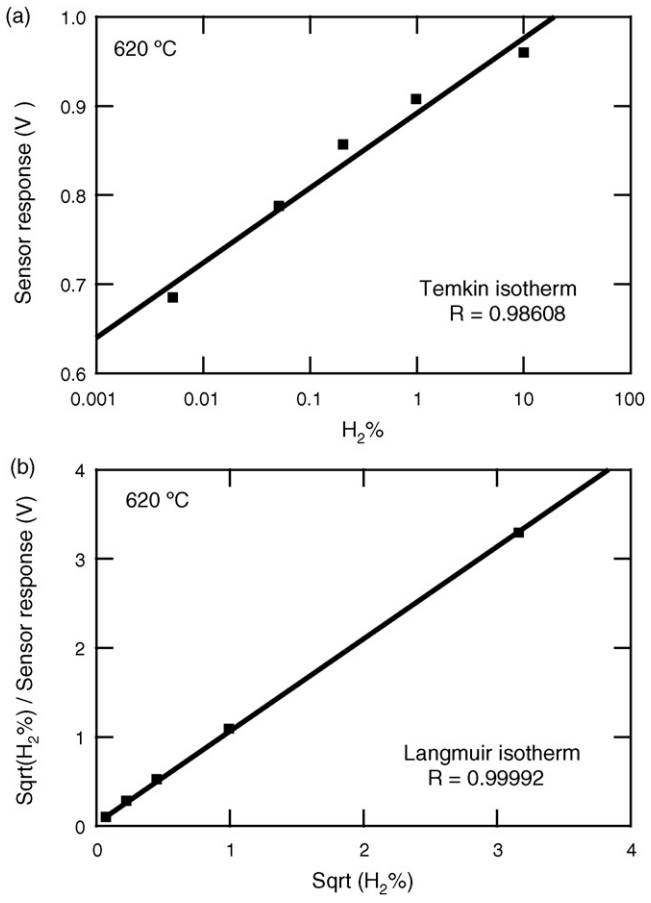

Fig. 6. Sensor response (ΔV) as a function of hydrogen concentration from the data in Fig. 4. Plotted are the linear best fits to the (a) Temkin and (b) Langmuir isotherms with correlations of $R = 0.98608$ and $R = 0.99992$, respectively.

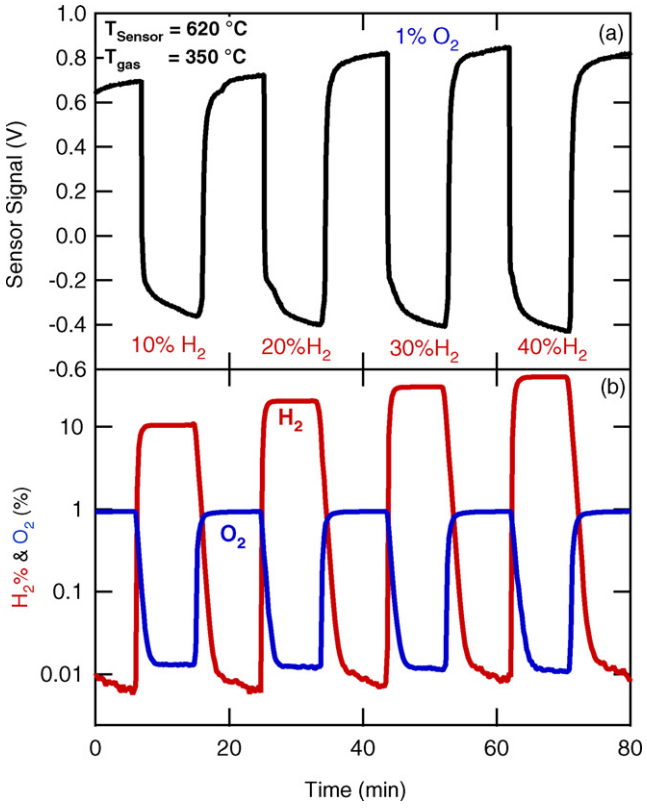

Fig. 7. (a) Sensor measurement in 10–40% H_2 gas with the sensor at 620 °C and flowing gas at 350 °C. The gas flow rate is 1000 sccm and 1% O_2 was used as the reference. (b) The mass spectrometer signal for both hydrogen and oxygen (the signal for the balance gas nitrogen is not shown). The SiC sensor results are completely validated by the mass spectrometry data.

The gas compositions selected for these investigations were designed to determine the range of operation of the hydrogen sensor as a potential monitor of syngas composition. Previous work on hydrogen sensors for energy plant applications has focused largely on either slightly oxidizing or slightly reducing gases. Syngas composition monitoring, however, requires use of reducing gas mixtures with considerable hydrogen content. As syngas also contains large fractions of carbon monoxide, it is important to determine to what extent the presence of carbon monoxide would interfere with the hydrogen concentration measurements. An additional contaminant of "clean" syngas is hydrogen sulfide, which is removed to reach SO_2 emissions levels required by government pollution limits. The typical level for sulfur in clean syngas is 200 ppm, as reported during early operations of the Tampa Electric IGCC plant in Tampa, FL during the year 2000 [24]. Our sensor was exposed to a 10 times higher H_2S concentration to determine if sulfur is fatal to device performance.

3.2.1. Sensor response 0.1–50% hydrogen

The sensor was first exposed to 0.1, 1, 2, 5, 10, 20, 30, 40 and 50% H_2 gas flows at 350 °C and a 1000 sccm flow rate. Note that the uncertainty is about ±0.5 for 2 and 5% hydrogen and could vary from 0.7–1.1% for 10–50% hydrogen gas. As in the laboratory, 1.02% O_2 was used as the reference gas. The sensor itself was maintained at the considerably higher temperature of 620 °C. This gas flow rate is about 10 times higher than what was used in the laboratory experiments. The device response to single pulses of 10, 20, 30 and 40% H_2 are shown in Fig. 7a. The SiC sensor results were validated with the simultaneous mass spectrometry data of Fig. 7b. There is a one-to-one correspondence between the mass spectrometer and SiC sensor measurements. The gas stream at the inlet to the mass spectrometer has cooled to near room temperature, as the instrument is located about 13 m downstream from the reactor and the SiC sensor. The mass spectrometer gives a reading of the gas composition averaged over a 13 s interval and provides one such measurement every 15 s. This is in stark contrast to the SiC device, which provides an essentially instantaneous (<10 ms) measurement of the 350 °C gas composition. The SiC sensor can detect transients in the gas composition that may be missed by time averaged measurements with other technique. Within the time synchronization of the two data collection systems, both systems report the same response to alternating pulses of hydrogen and oxygen.

We made the following important observation about the kinetics of hydrogen transduction of the SiC sensor while monitoring an energetic or heated gas stream. Although the flowing gas was maintained at 350 °C, as reported by the thermocouple 1 cm upstream from the sensor, the temperature of the sensor itself

decreased from 620 °C by 10–25 °C during the flow of high concentration hot hydrogen gas. The decrease in temperature was proportional to the H_2 concentration. This is not a new phenomenon; the dissociation of molecular hydrogen on a heated Pt surface to form atomic hydrogen is known to be an endothermic reaction consuming heat and causing the temperature of the Pt surface to decrease [25]. Our observations imply that the hydrogen gas and Pt catalytic film are not in thermal equilibrium, as energy is conserved in the process of hydrogen dissociation. Another factor to be considered would be the difference in thermal conductivity between hydrogen and nitrogen gas. Hydrogen has a much higher conductivity than nitrogen. It would result in a loss of more heat or a decrease in sensor temperature. Note these observations were possible because the sensor and the flowing gas had independent heating systems. Further work is needed to determine how to incorporate the energetics of hydrogen dissociation process into a model for sensor operation that does not evoke an isotherm.

The response of the sensor to 0.1, 1, 2, 5, 10, 20, 40 and 50% of H_2 is shown in Fig. 8. The data were obtained from analysis of the steady state response of the sensor to three pulses at each concentration. A logarithmic plot of the data using the Temkin isotherm gives a slope of 239.4 ± 0.4 mV/decade with a correlation of $R = 0.98304$, see Fig. 8a. The data is somewhat scattered and appears to be saturating for 30% H_2 and above. However, this saturation disappears when using the linearized Langmuir isotherm to plot the same data, see Fig. 8b. The scatter in the fit also decreases significantly, yielding a slope of 0.72 ± 0.02, and an intercept of 0.49 ± 0.10 with a correlation of $R = 0.99609$. The Langmuir isotherm provides a better to fit than the Tempkin isotherm to these sensor measurements in a heated gas stream, especially at high hydrogen concentrations. Note that there is a difference in slope between the data from the industrial experiments (Fig. 8) versus the laboratory measurements (Fig. 6), which we believe, is most likely due to the higher gas temperature gas (350 °C versus room temperature) and higher gas flow rate (1000 sccm compared to 80 sccm) in the high performance reactor. Further experiments are needed to verify our assumption that the SiC sensor response depends on the kinetic energy of the gas through the gas temperature, flow rate and pressure.

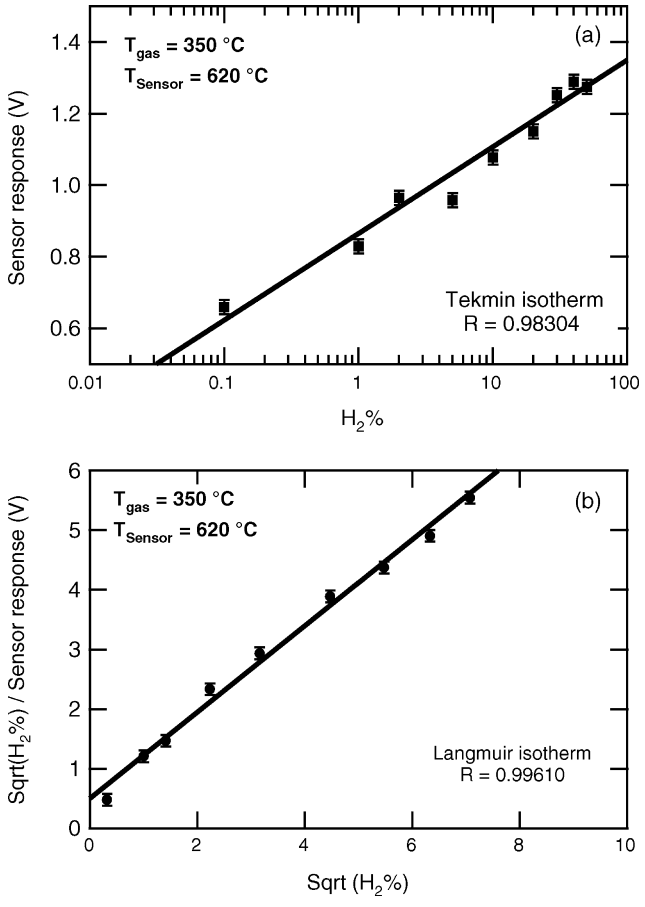

Fig. 8. Sensor response (ΔV) of the device in Fig. 6, with a 1000 μm diameter catalytic film to 0.1, 1, 2, 5, 10, 20, 30, 40 and 50% H_2. The sensor temperature is 620 °C while the gas temperature is 350 °C with a flow of 1000 sccm. Plotted are linear best fits to the (a) Temkin and (b) Langmuir isotherms with correlations of $R = 0.98304$ and $R = 0.99609$, respectively. The Langmuir isotherm provides a better fit, especially at high hydrogen concentration.

3.2.2. *Effect of common syngas interferants CO, CO_2 and CH_4*

Carbon monoxide (weak reducer), carbon dioxide (weak oxidizer) and methane (reducer) are three of the most common interferants encountered during syngas production. We examined their impact on the hydrogen response of the SiC gas sensor operating under industrial conditions (1000 sccm flow of 350 °C gas) for two scenarios. First, to understand the effect of interferants in slightly oxidizing or reducing environments, a low concentration of each interferant was individually introduced into a low concentration flow of H_2. Secondly, in order to simulate syngas composition monitoring with considerable hydrogen content, high concentrations of the individual interferants as well as combinations of the interferants were introduced into a gas steam with high H_2 content.

The first set of experiments, performed under slightly reducing conditions, is shown in Fig. 9. The sensor was exposed to 1% O_2 followed by 0.1% H_2 to establish the baseline signal. Then the response to pulses of 5% CO (Fig. 9a), 5% CH_4 (Fig. 9b) and 2.7% CO_2 (Fig. 9c) on top of 0.1% H_2 were recorded. All the measurements were made in a 1000 sccm flow of 350 °C gas with the sensor held at 620 °C. Note that under these measurement conditions CO and CH_4 are reducing species. The small spikes in the sensor signal near 19 min on trace 9a and 23 min on trace 9b are not the response of the sensor to the particular interferant, but are due to transients in the gas mixing system (see gas flow schematic in Fig. 2) as reported by the on-line mass spectrometer. Therefore, the introduction of low concentration of CO, CO_2 and CH_4 had no significant effect on the ability of the SiC sensor to monitor hydrogen in a slightly reducing environment.

The second scenario looked at the effect of carbon monoxide, carbon dioxide and methane both individually and in combination under "typical" syngas operating conditions. Using a 20% H_2 gas mixture (1000 sccm gas flow at 350 °C, with $T_{sensor} = 620$ °C) we sequentially introduced 5% CH_4, 40% CO_2 and 40% CO into the gas stream according to the schematic in

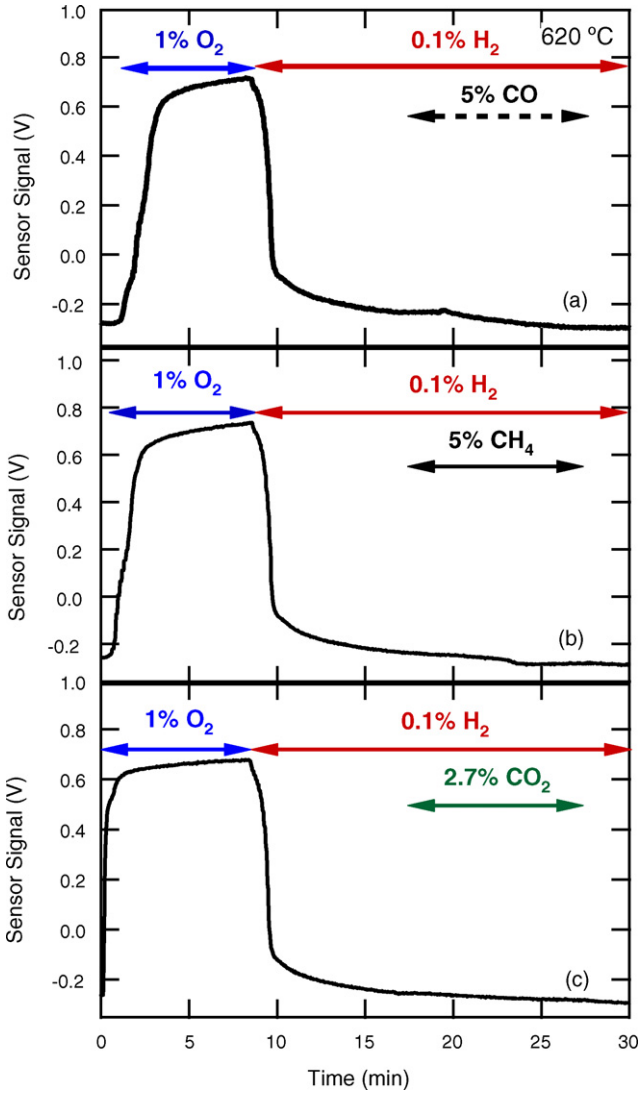

Fig. 9. Sensor response to pulses of the interferants (a) 5% CO, (b) 5% CH_4 and (c) 2.7% CO_2 under slightly reducing conditions. The measurement was made under industrial conditions with a 1000 sccm 0.1% H_2 gas stream at 350 °C, with T_{sensor} = 620 °C. The interferant pulse was introduced into the hydrogen gas stream at ~19 min and then removed at~28 min. The interferants had a negligible effect on the hydrogen monitoring capability of the SiC sensor.

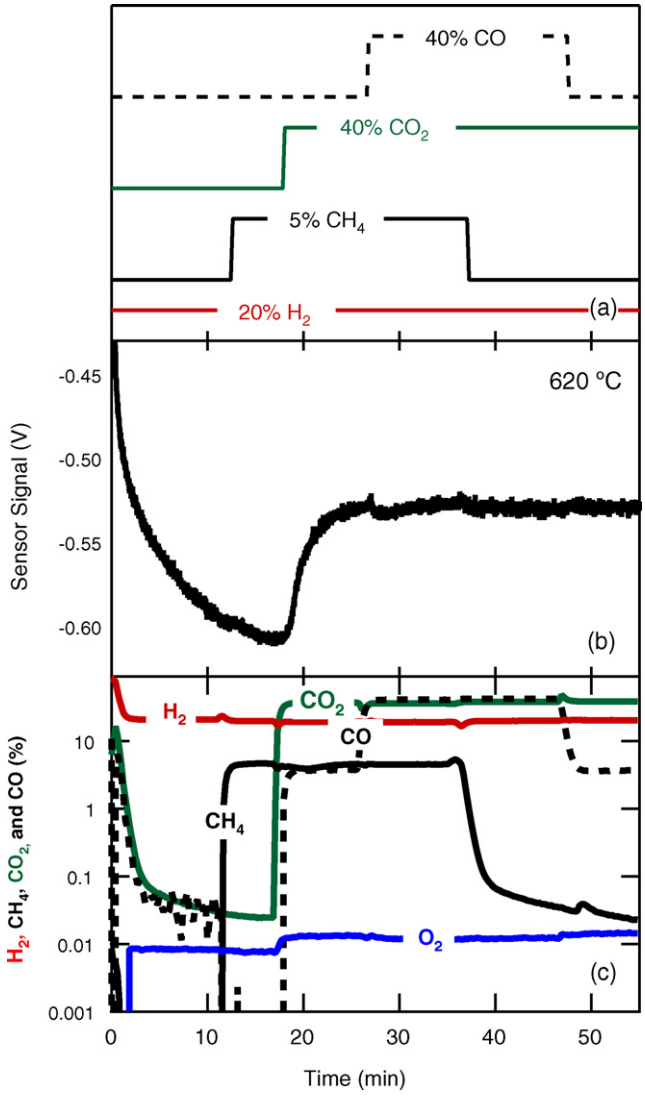

Fig. 10. Performance of the SiC sensor as a hydrogen monitor under "typical" fuel reforming conditions. (a) Schematic of the input gas flow sequence, showing sequential injection of 5% CH_4/95% N_2, 40% CO_2/60% N_2 and 40% CO/60% N_2 on top of a base line 20% H_2/80% N_2 gas stream, (b) SiC sensor response to the "standard" interferants, CH_4, CO_2 and CO on a 350 °C, 20% H_2 gas flow at 1000 sccm with the sensor at 620 °C and (c) in-line mass spectrometer signal of the gas composition inside the measurement chamber (the signal for the balance gas N_2 is not shown in this and subsequent figures). Methane and carbon monoxide have a negligible (<0.03%) effect on the sensor response to hydrogen.

Fig. 10a. As in all of our measurements the balance gas is N_2. During the period from 27 to 36 min all three interferants were pumped simultaneously into the HPR. Starting at time 36 min, methane then carbon monoxide was removed leaving only carbon dioxide in the hydrogen gas stream. The output of the SiC sensor is given in Fig. 10b. Note that the vertical axis has been greatly magnified, covering a range of only 200 mV as compared to ΔV = 1150 mV, the measured response to 20% H_2 from Fig. 8, to highlight the relatively small effect of the interferants. The mass spectrometer signal from H_2, CO_2, CO, CH_4 and O_2 are shown in Fig. 10c, where the relative concentration in percent for each species is referenced with respect to the total gas composition of the system. Note that as nitrogen is used as the balance gas for all of the gas mixtures, we do not show the nitrogen signal in the mass spectrometer data.

The reducer 5% CH_4 and weak reducer 40% CO had no noticeable effect on the SiC sensor response either upon introduction or upon removal from the reducing 20% H_2 gas stream. The response of the sensor to 20% H_2 is ~1150 mV and the noise in the sensor output, from Fig. 10b, about ±3 mV. Therefore any effect of methane or carbon monoxide is on the order of a few tenths of a percent of the hydrogen signal.

Addition of the oxidizer 40% CO_2 changed the sensor signal by 7% towards a more oxidizing gas composition. According to the following two reactions this is reasonable result:

$$CO_2 + H_2 \Leftrightarrow CO + H_2O \quad (3)$$

$$CO + 2H_2 \Leftrightarrow CH_4 + (1/2)O_2 \quad (4)$$

In hydrogen gas stream addition of CO_2 will always produce CO; the mass spectrometer indicates that that the amount of CO produced is about 6% of the total gas composition in the system. The second reaction indicates that the CO in turn produces about 0.02% of O_2 (of the total gas composition) as a by-product. This implies that adding CO_2 to a hydrogen gas flow will always generate CO and a smaller amount of O_2. At this point, we cannot determine whether the 7% change in sensor signal upon introduction of CO_2 is this direct response to CO_2 or a secondary response to the generation of O_2 as a by-product.

The purpose of the next experiment on the 20% H_2 gas stream was to confirm the expected behavior, based on the reactions given in Eqs. (3) and (4), of an isolated pulse of 40% CO as well as to determine the reproducibility of the sensor response to a series of 40% CO_2 pulses. A schematic of the gas pulses is given in Fig. 11a, the sensor signal in Fig. 11b and the mass spectrometer signal in Fig. 11c. Again, the vertical scale of the sensor signal has been magnified to encompass only 140 mV, the response to 20% H_2 is $\Delta V = 1150$ mV, to highlight the small effect of the interferants. From the first pulse, introduction of CO into the system generated CH_4 and O_2 as expected according to Eq. (4). The SiC sensor reports that the gas content of the gas in the system is slightly less reducing, as indicated by a change in the slope of the signal. Upon introduction of CO_2 in pulses 2, 3 and 4, we observe the simultaneous creation of CH_4, O_2 and CO (at the level of 0.001%, ~0.02% and ~4% according to the mass spectrometer) as expected from Eqs. (3) and (4). The response of the SiC sensor to the CO_2 pulses is a 7% change from the signal level in hydrogen, with a repeatability of ±2%. Note that the apparent spikes in CO mass spectrometer concentration (black dashed line) when the CO_2 flow is turned off may be at least partly mathematical artifacts produced by the response of the mass spec software to changes in the gas stream composition during the 13 s sampling cycle. Again, we cannot distinguish if this direct response is due to CO_2 or a secondary reaction due to generation of O_2 as a by-product.

From these last two experiments, we find that neither methane nor carbon monoxide, as individual constituents or in combination, affect the hydrogen monitoring capabilities of our SiC sensor, within the signal to noise ratio of our measurement system. However, CO_2 does have an oxidizing effect, resulting in a 7% change in the sensor signal. At this point it is not known whether this is a primary or secondary reaction. Further experiments have been designed to clarify this issue.

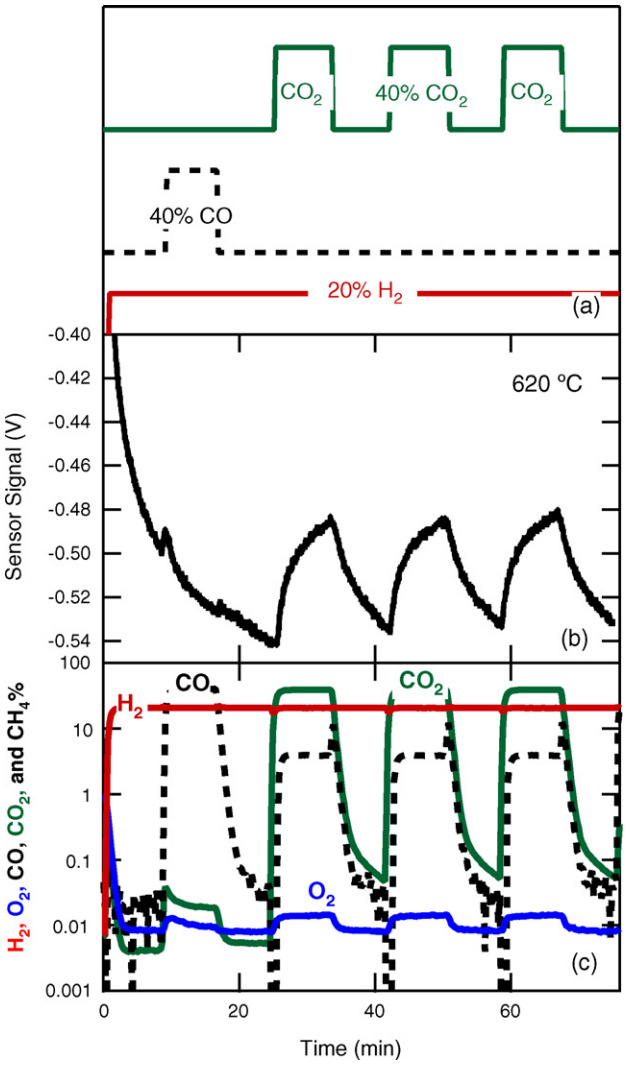

Fig. 11. Performance of the SiC sensor as a hydrogen monitor, while subjected to pulses of 40% CO and 40% CO_2. (a) Schematic of the input gas flow sequence, showing injection of a single pulse of 40% CO/60% N_2, followed by three pulses of 40% CO_2/60% N_2 on top of a base line 20% H_2/80% N_2 gas stream, (b) response of the sensor to CO and CO_2 pulses while monitoring a 350 °C, 20% H_2 flow at 1000 sccm with $T_{sensor} = 620$ °C and (c) the mass spectrometer signal of the gas composition inside the measurement chamber. The sensor performance is not directly affected by CO; it is not known whether the effect of CO_2 is due to a primary or secondary reaction.

3.2.3. *Effect of sulfur contamination*

The presence of sulfur contamination presents a challenge in terms of monitoring coal-based combustion processes as devices with refractory metal catalytic sensing films can be poisoned by species such as H_2S. In this experiment we introduced a ~2000 ppm H_2S pulse on a 1000 sccm 10% H_2 gas flow at 370 °C as shown in Fig. 12a. The SiC sensor signal is shown in Fig. 12b for $T_{sensor} = 600$ °C, along with the mass spectrometer signal in Fig. 12c. We have amplified the vertical axis in Fig. 12b to 140 mV to highlight the relatively small change due to sulfur. The sensor response to 10% H_2 is $\Delta V \sim 1000$ mV, whereas introduction of H_2S into the hydrogen gas stream produced only a 115 mV positive, or oxidizing, signal. There are two extraneous features in the data that are not part of the sulfur experiment. First, the small hump on the left wing of the sensor signal at around 3 min is to be ignored as it comes from residual CO_2 in the gas flow line (Fig. 2 shows that CO_2 shares a common line with H_2S). Secondly, in the mass spectrometer trace the four spikes in the H_2 and H_2S signals between 18 and 35 min are not from our experiment, but due to gas grabs in front of the mass spectrometer (see Fig. 2) for a separate concurrent experiment.

Following these measurements, the sensor module was purged with 1% oxygen for ~22 min to remove H_2S from the

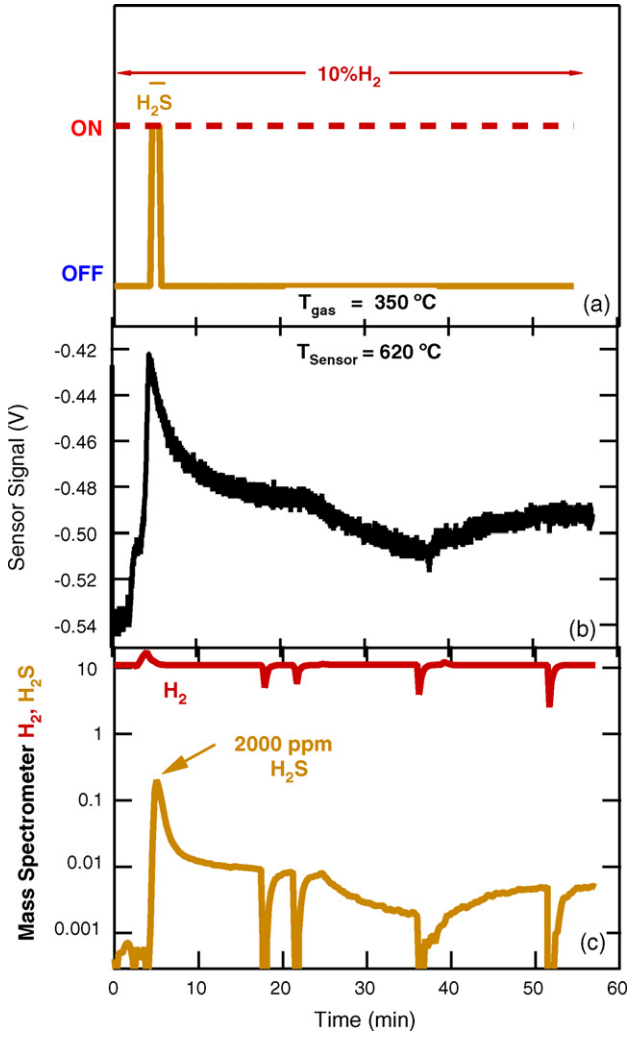

Fig. 12. The effect of a large (2000 ppm) sulfur pulse on the hydrogen monitoring capabilities of the SiC sensor. Under "typical" fuel reforming conditions, the gas stream contains 200 ppm of H_2S. (a) Schematic of the gas flow showing injection of a single pulse of 2000 ppm H_2S/99.80% N_2 on top of a 10% H_2/90% N_2 gas stream, (b) the sensor signal for a 370 °C gas stream with T_{sensor} = 620 °C and (c) the mass spectrometer signal of the gas composition inside the measurement chamber. The device is not poisoned by sulfur.

system. However, as we are using a stainless steel reaction vessel, it is possible that the sulfur adsorbs to the inner walls and continues to desorb over time, thereby affecting any subsequent measurements performed in this module. Due to limited experimental time in the high performance reactor, it was not possible to test the sensor performance after sulfur exposure at NETL. Upon returning to MSU the sensor response as a function of hydrogen concentration was measured over 2.5 decades with a room temperature H_2 gas stream, in the original test module. The sensor response, analyzed using the Tempkin isotherm, is a factor of three higher after high-temperature gas exposure as compared with the original device response in Fig. 4. We postulate that exposure to a high-temperature gas stream at NETL further activated the Pt catalytic sensing film. No degradation in the performance of the device as a hydrogen sensor was observed following a large (2000 ppm) dose of H_2S that is a factor of 10 higher than the typical level of sulfur for clean syngas [24].

4. Conclusion

We have designed and built a high-temperature gas sensing module for laboratory scale testing that is also capable of monitoring gases in harsh industrial environments, such as an energy plant. The sensor is a catalytic gate field-effect device (Pt–SiO_2–SiC) that can detect hydrogen-containing species in chemically reactive, high-temperature environments in real time. We have demonstrated the long-term reliability of our SiC sensor and the robustness of the sensor packaging technology; all the measurement in this paper are from a single device which were obtained during a 5-day industrial measurement cycle, followed by more than 400 h of continuous operation under laboratory conditions. The data were taken in a 350 °C flowing gas stream to achieve conditions that were closer to those found in a coal gasifier as compared to using room temperature gas. The sensor temperature of 620 °C was independently set to well above that of the gas under interrogation for output stability, as well as to maximize the magnitude and speed of the sensor response.

The SiC sensor has a large dynamic range, the lower bound of the sensitivity is at least 52.1 ppm, and the same device was also used to monitor a 50% H_2 gas stream. The linearized Langmuir isotherm was successfully used to model the sensor response for both high temperature and room temperature hydrogen. The potential for using the SiC sensor to monitor hydrogen in a coal gasification application was investigated by looking at the effect of common interferants on the device response to a 20% hydrogen stream. Carbon monoxide and methane at the 40 and 5% level, respectively had no measurable effect on the sensor within the S/N ratio. A 7% change in the sensor signal was observed for a 40% carbon dioxide gas stream; however it is not known whether this is a direct response to CO_2 or oxidizing by-products. Hydrogen sulfide, which can be deadly for refractory metal catalysts, such at our Pt sensing film, did not poison the sensor performance at the 2000 ppm level, which is 10 times higher than at an operating power plant. All of these sensor measurements were validated using an in-line mass spectrometer.

The series of measurements performed under industrial conditions showed that the SiC sensor could be a very valuable tool for real time monitoring and feedback of combustion processes, as it instantly reported any changes in the "net" hydrogen content of the gas stream. For example, changes in the gas composition due to the generation of by-products, release of residual gas in the gas mixing system, accidental opening of a gas switch were immediately observed in the sensor signal, then validated some time later by the mass spectrometer output.

We have demonstrated the capabilities of a SiC device as a hydrogen sensor to monitor the performance of a fuel reforming or syngas production application. Other potential applications for this reliable and robust MOS SiC gas sensor include monitoring syngas fuel gas flow to a turbine or a high-temperature fuel cell, emissions control in automobiles, feedback control during mixing of air and fuel in an internal combustion engine and the detection of flame fronts in controlled experiments.

Acknowledgments

The authors acknowledge the contribution of Peter Tobias, currently at Honeywell. The gate oxidation was performed by John Williams, Dept. of Physics, Auburn University. The devices were fabricated in the W.M. Keck Microfabrication Facility at Michigan State University. The high performance reactor is managed by Dushyant Shekawat, DOE National Energy Technology Lab, Morgantown, WV. The data acquisition program was developed by Nathan Verhanovitz. The sensor test module was fabricated by James Muns, Thomas Palazzolo and Thomas Hudson, Dept. of Physics Machine Shop, Michigan State University.

This article was prepared with the support of the U.S. Departments of Energy (DOE), under Award No. DE-FC26-03NT41847. However, any opinions, findings, conclusions, or recommendations expressed herein are those of the authors and do not necessarily reflect the view of the DOE.

References

[1] A.L. Spetz, S. Savage, Advances in SiC field effect gas sensors, in: W.J. Choyke, H. Matsunami, G. Pensl (Eds.), Silicon Carbide: Recent Major Advances, Springer-Verlag, Berlin, 2004, pp. 869–896.
[2] A.L. Spetz, L. Unéus, H. Svennningstorp, P. Tobias, L.G. Ekedahl, O. Larsson, A. Göras, S. Savage, C. Harris, P. Mårtensson, R. Wigren, P. Salomonsson, B. Häggendahl, P. Ljung, M. Mattsson, I. Lundström, SiC based field effect gas sensors for industrial applications, Phys. Stat. Solidi A 185 (2001) 15–25.
[3] P. Tobias, B. Golding, R. Ghosh, Interface states in high temperature gas sensors based on SiC, IEEE Sens. J. 3 (2003) 543–547.
[4] J. Schalwig, P. Kreisl, S. Ahlers, G. Müller, Response mechanism of SiC-based MOS field-effect gas sensors, IEEE Sens. J. 2 (2002) 394–402.
[5] S. Nakagomi, A.L. Spetz, I. Lundstöm, P. Tobias, Electrical characterization of carbon monoxide sensitive high temperature sensor diode based on catalytic metal gate–insulator–silicon carbide structure, IEEE Sens. J. 2 (2002) 379–386.
[6] S. Kanadasamy, A. Trinchi, W. Wlodarski, E. Comini, G. Sberveglieri, Hydrogen and hydrocarbon gas sensing performance of Pt/WO_3/SiC MROSIC devices, Sens. Actuator B 111 (2005) 111–116.
[7] A. Arbab, A. Spetz, Q. Wahab, M. Willander, I. Lundström, Chemical sensor for high temperatures based on silicon carbide, Sens. Mater. 4 (1993) 173–185.
[8] A. Baranzahi, A.L. Spetz, I. Lundström, Reversible hydrogen annealing of metal–oxide–silicon carbide devices at high temperatures, Appl. Phys. Lett. 67 (1995) 3203–3205.
[9] R.N. Ghosh, P. Tobias, H. Hu, M. Koochesfahani, Fast solid state gas sensor characterization technique with millisecond resolution, Proc. IEEE Sens. (2005) 1411–1413.
[10] A. Salomonsson, M. Eriksson, H. Dannetun, Hydrogen interaction with platinum and palladium metal–insulator–semiconductor devices, J. Appl. Phys. 98 (2005) 014505-1–014505-10.
[11] C.C. Cheng, Y.Y. Tsai, K.W. Lin, H.I. Chen, C.T. Lu, W.C. Liu, Hydrogen sensing characteristics of a Pt–oxide–$Al_{0.3}Ga_{0.7}As$ MOS Schottky diode, Sens. Actuator B 99 (2004) 425–430.
[12] I. Lundström, Why bother about gas-sensitive field-effect devices, Sens. Actuator A 56 (1996) 75–82.
[13] I. Lundström, L.G. Petersson, Chemical sensors with catalytic metal gates, J. Vac. Sci. Technol. A 14 (1996) 1539–1545.
[14] J. Fogelberg, M. Eriksson, H. Dannetun, L.G. Petersson, Kinetic modeling of hydrogen adsorption/absorption in thin films on hydrogen-sensitive field-effect devices: observation of large hydrogen-induced dipoles at the Pd–SiO_2 interface, J. Appl. Phys. 78 (1995) 988–996.
[15] L.G. Petersson, H.M. Dannetun, J. Fogelberg, I. Lundström, Hydrogen adsorption states at the external and internal palladium surfaces of a palladium–silicon dioxide–silicon structure, J. Appl. Phys. 58 (1985) 404–413.
[16] K. Scharnagl, A. Karthigeyan, M. Burgmair, M. Zimmer, T. Doll, I. Eisele, Low temperature hydrogen detection at high concentrations: comparison of platinum and iridium, Sens. Actuator B 80 (2001) 163–168.
[17] A.E. Åbom, R.T. Haasch, N. Hellgre, N. Finnegan, L. Hultman, M. Eriksson, Characterization of the metal–insulator interface of field-effect chemical sensors, J. Appl. Phys. 93 (2003) 9760–9768.
[18] S. Nakagomi, T. Azuma, Y. Kokubun, Hydrogen gas response of Pt–thin SiO_2–SiC Schottky diode in the presence of oxygen, Electrochemistry 70 (2002) 174–177.
[19] S. Dhar, S.R. Wang, J.R. Williams, Interface passivation for silicon dioxide layers on silicon carbide, MRS Bull. 30 (2005) 288–292.
[20] R. Ghosh, P. Tobias, SiC field-effect devices operating at high temperature, J. Electron. Mater. 34 (2005) 345–350.
[21] D. Shekhawat, D. Berry, T.H. Gardner, Diesel fuel reforming kinetics, Office of Fossil Energy Fuel Cell Program, FY 2005 Annual Report, 2005, pp. 171–176.
[22] R.N. Ghosh, R. Loloee, T. Isaacs-Smith, J.R. Williams, High temperature reliability of SiC n-MOS devices up to 630 °C, Mater. Sci. Forum 527–529 (2006) 1039–1042.
[23] H. Katsuta, R.B. McLellan, Diffusibity, permibility and solubility of hydrogen in platinum, J. Phys. Chem. Solids 40 (1979) 697–699.
[24] U.S. Department of Energy, Office of Fossil Energy, The Tampa Electric Integrated Gasification Combined-Cycle Project: An Update, Topical Report 19, July 2000.
[25] Vecco Application Note No. 1/96, Cracking efficiency of the Vecco atomic hydrogen source, St. Paul, MN, January 1996 (online) http://www.veeco.com/appnotes/96_JAN_atom-H%20(11-04).

Biographies

Reza Loloee received the PhD degree in materials science engineering from Michigan State University in 2000. He has worked as a materials specialist at Department of Physics and Astronomy, Michigan State University since 1989.

Benjamin T. Chorpening received the BS in mechanical engineering degree from Ohio University in 1993, and the MS and PhD degrees in mechanical engineering from the University of Illinois, Urbana-Champaign in 1995 and 2000. After graduation, he worked as a postdoctoral researcher at Sandia National Laboratories for 2 years, and then joined the research staff at the National Energy Technology Laboratory in Morgantown, WV, in 2002. His current research is on sensors and combustion technology for advanced power generation systems, particularly turbines.

Stephen Beer acquired a BS in physics from the University of Pittsburgh in 1971 and an MS in nuclear physics from West Virginia University in 1976. He is currently involved in thermal imaging of combustors and mass spectrometer characterization of catalysis gas streams at the National Energy Technology Laboratory in Morgantown, WV.

Ruby N. Ghosh received the BA degree in physics from Swarthmore College in 1982, the MS and PhD degrees in applied physics from Cornell University in 1986 and 1991. She did her postdoctoral research at the National Institute for Standards and Technology, USA. From 1994 to 1996 she was a member of technical staff at Bell Laboratories, Lucent Technologies, USA. In 1996 she joined the Department of Physics at Michigan State University, USA, where she is a research associate professor in the Physics Department. Her current research interests are in optical and semiconductor devices for sensing applications and the physics of electronic transport in mesoscopic structures.